JOURNAL OF APPLIED ELECTROCHEMISTRY **28** (1998) 1213–1219

Influence of the forming electrolyte on the electrical properties of tantalum and niobium oxide films: an EIS comparative study

G. E. CAVIGLIASSO, M. J. ESPLANDIU, V. A. MACAGNO

INFIQC, Departamento de Fisicoquímica, Facultad de Ciencias Químicas, Universidad Nacional de Córdoba, Agencia Postal 4, Casilla 61, 5000 Córdoba, Argentina

Received 6 October 1997; accepted in revised form 23 December 1997

The electrochemical oxidation of Ta and Nb and the dielectric behaviour of the oxide films thus formed were investigated in the following electrolytes: H_2SO_4, HNO_3, H_3PO_4 and NaOH. Characterization of the films was carried out by means of potentiodynamic current–potential profiles (in the range 0–8 V) and electrochemical impedance spectra (in the range 0.1 Hz–100 kHz). The a.c. response of the oxide films was modelled as a single layer structure on the basis of an equivalent circuit with constant phase elements (CPE). The dependence of the oxide resistance and oxide capacitance with potential is also reported.

Keywords: *anodic oxide films*, *tantalum*, *niobium*, *impedance spectroscopy*, *dielectric behaviour*

1. Introduction

Research on the electrochemical behaviour of oxide films on Ta and on Nb is vast and has covered a wide range of topics, such as anodic film growth and breakdown [1–14], composition [1], dielectric properties [15–19], stability and corrodability [20–23], electron transfer [24, 25], photoelectrochemistry and optical properties [26–30] and electrochromism [31–33]. A number of comparative studies have been reported. Hornkjol investigated the passive behaviour of anodic oxide films on Ta and on Nb by means of galvanostatic growth along with long-time potentiostatic polarization [14]. Randall *et al.* carried out a radiotracer study of the film compositions emphasizing anion incorporation from the forming electrolyte [1]. Al-Kharafi and Badawy used electrochemical impedance spectroscopy (EIS) for testing the dielectric behaviour of H_3PO_4 passivated Ta and Nb [23].

The analysis of the dielectric properties, especially the effect of the forming electrolyte on the oxide characteristic parameters (resistivity and dielectric constant) has been sparingly dealt with. Macagno and Schultze [15] performed single frequency measurements to assess the pH-dependence of the Ta/Ta_2O_5 capacitance. EIS and XPS (X-ray photoelectron spectroscopy) experiments were carried out by Kerrec *et al.* for the characterization of the stoichiometry and dielectric behaviour of Ta anodic oxides grown in H_2SO_4 [19]. The frequency and temperature dependence of the impedance for Ta samples anodized in Na_2SO_4 was analysed by Resetic and Jaric [18]. Capacitance-formation potential relationships were evaluated by Young [34] in his study of the anodic polarization of Nb in H_2SO_4 and Na_2SO_4.

In spite of the work already done, there remain a number of questions concerning the influence of the forming electrolyte on the dielectric behaviour of Ta/Ta_2O_5/electrolyte and Nb/Nb_2O_5/electrolyte systems, which have yet to be addressed. The aim of this work is to investigate the electrical properties of oxide films electrochemically grown on Ta and on Nb in different electrolytes.

Potentiodynamic growth profiles and electrochemical impedance spectra are used for the characterization of the anodic oxide films. The a.c. response is analysed and interpreted in terms of an equivalent circuit model and the variation of the electrical parameters with potential is discussed.

2. Experimental details

A three-compartment cell was used for the electrochemical experiments. The counter electrode was a platinum spiral and the reference electrode was a saturated calomel electrode (SCE). The working electrodes were discs of Ta (6.40 mm diam.) and of Nb (6.35 mm diam.) fixed in a Teflon holder. The electrode pretreatment procedures consisted of mechanical polishing with 400 grade emery paper, followed by chemical polishing with a HF (48%): HNO_3 (65%) : H_2SO_4 (98%) mixture in a 2 : 2 : 5 ratio. The stoichiometry of both the spontaneously and the anodically formed oxide layers was assumed to be Ta_2O_5 and Nb_2O_5 [10, 13, 15]. Capacitance measurements were performed in order to know the roughness factor of the electrodes pretreated with different polishing procedures. Thus, the roughness factor for both Ta and Nb electrodes was 1.1 estimated on the basis of a value of 1.0 for mechanically

0021-891X © 1998 Chapman & Hall

polished electrodes (up to 0.05 μm Al_2O_3), the same value obtained with electropolished surface electrode taken as reference [15].

The electrolytes used for electrochemical experiments were 0.5 M H_2SO_4, 1 M HNO_3, 1 M H_3PO_4 and 1 M NaOH. Measurements were carried out at room temperature (25 °C).

The electronic equipment comprised a potentiostat (Wenking LB 75 M or Heka PG 284/IEC), a waveform generator (EG&G 175) and an X–Y recorder (Hewlett Packard 7004B or Houston 2000). The EIS measurement were performed with an impedance spectrum analyzer Zahner IM5D. The amplitude of the perturbation signal was 20 mV and the frequency range was 0.1 Hz–100 kHz.

3. Results and discussion

3.1. *Growth of anodic oxide films*

The oxide growth on Ta and on Nb substrates was carried out by applying a cyclic potential sweep in the range 0–8 V at 0.1 V s^{-1}. Figures 1 for Ta and Fig. 2 for Nb show the potentiodynamic profiles obtained in the different electrolytes used for forming the films. In each case, the current–potential (i/E) profile shows the typical features of the behaviour of a valve metal subjected to a potential-time (E/t) triangular perturbation. The i/E profiles presented here closely resemble those already reported [15]. The forward scan is characterized by the appearance of a steady-state current (i_s) plateau after an initial step increase of current. This is associated with the growth of oxide according to a high field mechanism [15, 35–38]. Upon reversing the potential scan, the current decreases abruptly until it eventually reaches a constant value which is several orders of magnitude lower than that of i_s. This behaviour can be considered to be the result of a 100% current efficiency during oxide growth under potentiodynamic conditions [38], since no other electrochemical reaction occurs when the oxide growth reaction stops.

The higher initial value of the current in NaOH solutions in comparison with acidic electrolytes is a consequence of the shift of the beginning of oxide growth to more negative potentials as pH increases [15].

The use of HNO_3 as a forming electrolyte for valve metal oxides usually leads to film breakdown as evidenced by a substantial increase in the current which departs from its steady state value [39]. However, the i/E profiles for Ta and for Nb are remarkably similar regardless of the forming electrolyte, indicating that Ta_2O_5 and Nb_2O_5 are highly resistant to the aggresive action of HNO_3.

Table 1 shows the values of the anodization coefficient α calculated from the steady state current according to the equation

$$\alpha = \frac{i_s M}{nFv\delta_{ox}} \tag{1}$$

where v is the potential sweep, M is the oxide molecular weight, n is the number of electron exchanged

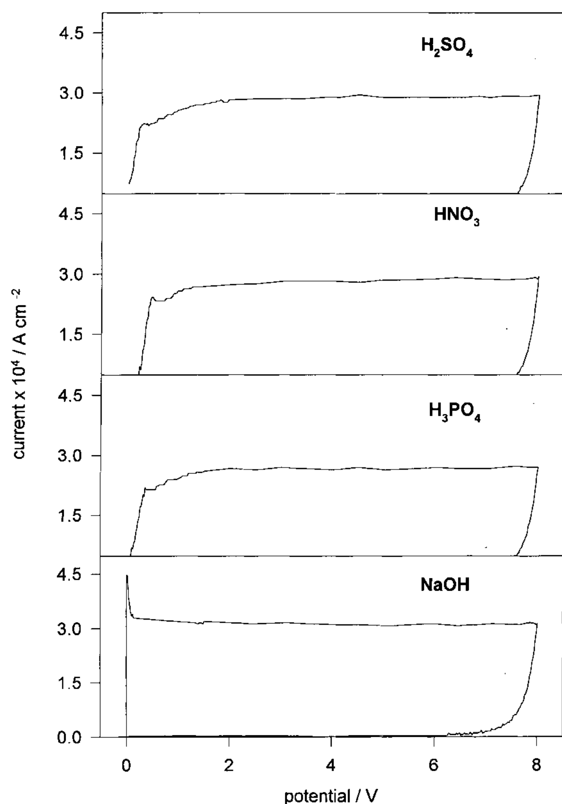

Fig. 1. Potentiodynamic i/E profiles at 0.1 V s^{-1} for Ta oxide films in different electrolytes.

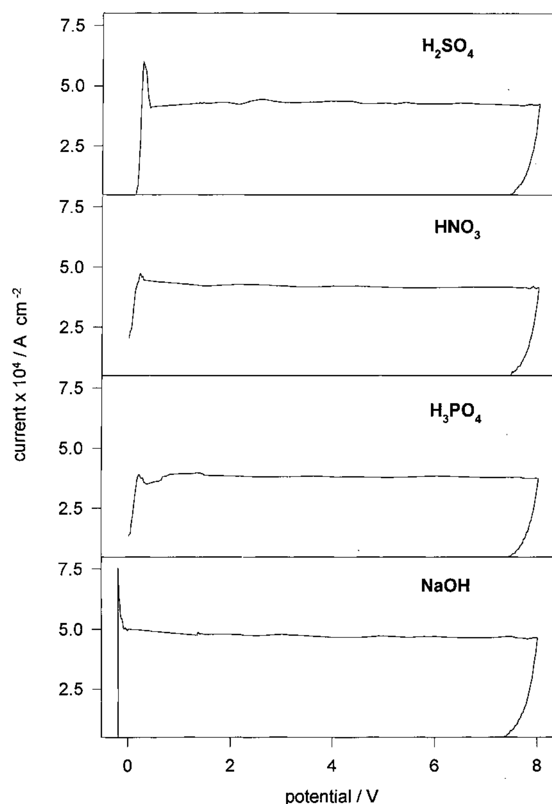

Fig. 2. Potentiodynamic i/E profiles at 0.1 V s^{-1} for Nb oxide films in different electrolytes.

Table 1. Anodization coefficients α/nm V^{-1}

Electrolyte	*Ta/Ta$_2$O$_5$*	*Nb/Nb$_2$O$_5$*
H_2SO_4	1.54 ± 0.04	2.35 ± 0.06
HNO_3	1.50 ± 0.04	2.15 ± 0.05
H_3PO_4	1.42 ± 0.04	1.98 ± 0.05
NaOH	1.65 ± 0.06	2.40 ± 0.06

(in this case $n = 10$), F is the Faraday constant and δ_{ox} is the density of the oxide. This equation is derived taking into account the high-field law for the oxide growth under potentiodynamic perturbations [15, 35–38]. It was assumed an oxide density of 4.47 g cm^{-3} and 8.2 g cm^{-3} for Nb and Ta oxides respectively, that is, the values for crystalline oxides.

The coefficients values are in good agreement with those reported in the literature [10, 13–15, 19, 22]. Oxides grow thicker in NaOH than in acidic electrolytes, since HO^- adsorption at the oxide/electrolyte interface hinders the incorporation of any other anion, thus enhancing ion conduction and transfer through the oxide film [35]. The higher α values observed for Nb oxides with respect to those for Ta oxides are related to the greater i_s and lower oxide density of Nb_2O_5 [38].

3.2. *Electrochemical impedance spectroscopy*

Oxide films on valve metals are, in general, non-homogeneous and amorphous [35]. Therefore, the interfacial impedance of an oxide layer on a substrate in contact with an electrolyte, is more realistically described by a transfer function which includes CPE [39–42].

$$Z(\omega) = \frac{R_L}{1 + (i\omega)^n R_L C_L} + R_s \qquad (2)$$

where R_L and C_L are the layer resistance and the layer capacitance, respectively; R_s is the solution resistance; $\omega = 2\pi f$ is the angular frequency; and $i = \sqrt{-1}$.

The impedance of a CPE is

$$Z_{CPE} = \frac{1}{(i\omega)^n C_L} \qquad (3)$$

the behaviour of an ideal capacitor dielectric being represented by $n = 1$. The structure may be schematicaly represented by the equivalent circuit of Fig. 3.

Figures 4, 5, 6 and 7 show impedance spectra recorded at 0.1 V, after the oxide growth. At this potential the current stabilizes in a few minutes, falling to values lower than 10 nA cm^{-2}. Measurements were not carried out at potentials below 0.1 V in order to avoid the hydrogen evolution reaction. At potentials equal to, or greater than, 0.1 V the impedance was found to be independent of the electrode potential. Solid lines represent the best complex nonlinear least-square (CNLS) fitting of the experimental data according to a single layer structure – equivalent circuit model considering CPE (Equation 2, Fig. 3).

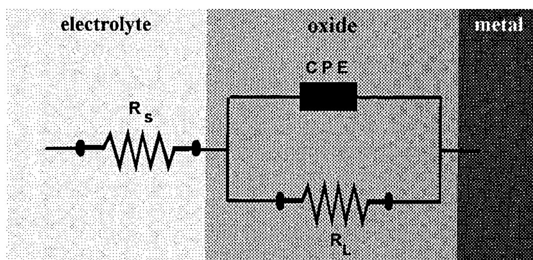

Fig. 3. Equivalent circuit model used in CNLS fitting.

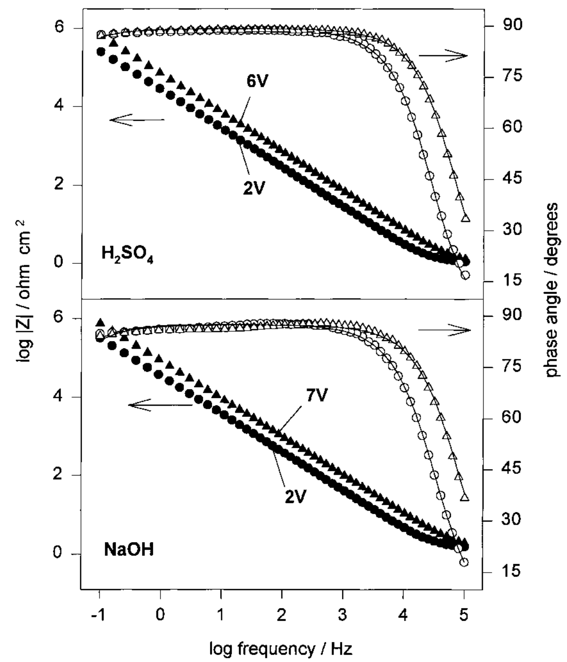

Fig. 4. Impedance spectra for Ta oxide films grown up to different formation potentials. Solid lines represents the fit to a single layer model.

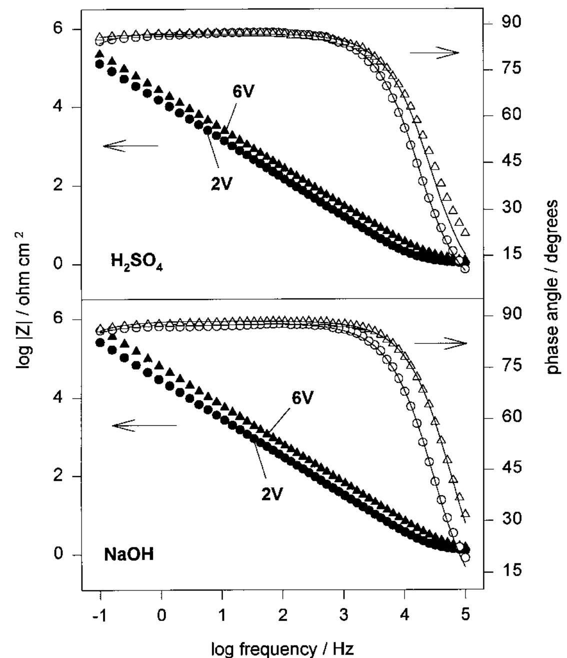

Fig. 5. Impedance spectra for Nb oxide films grown up to different formation potentials. Solid lines represents the fit to a single layer model.

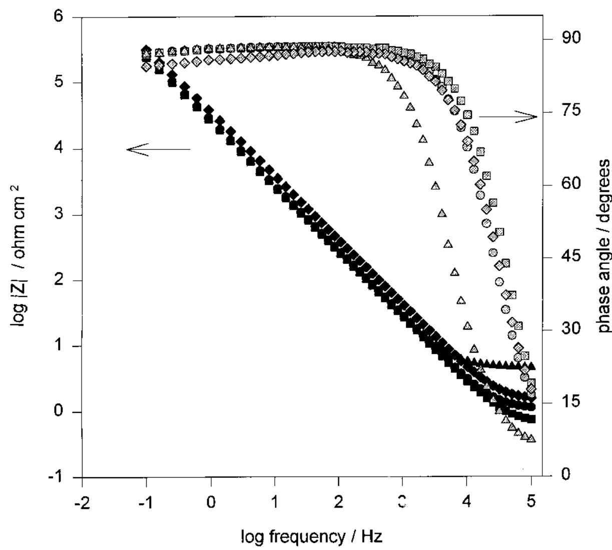

Fig. 6. Comparative impedance spectra for Ta oxide films grown in different forming electrolytes. Legend: (●) H_2SO_4, (■) HNO_3, (▲) H_3PO_4 and (♦) NaOH. (Ta/Ta_2O_5, $E_f = 2$ V).

Figure 4 for Ta and Fig. 5 for Nb show EIS results for oxide films of different thickness, grown in H_2SO_4 and in NaOH. Very similar results were found in the case of HNO_3 and H_3PO_4. The log $|Z|$ against log f curves show a linear relation and the phase angle (ϕ) has values close to 90° (at log $f < 3$ values). This is characteristic of a predominantly capacitive behaviour. The effect of increasing the final formation potential is observed only in the form of a log $|Z|$ increase corresponding to a greater film thickness.

The analysis of the CPE parameter n (Table 2) and the phase angle (Table 3) values (obtained from the CNLS fitting) indicates that the dielectric behaviour of the anodic Ta and Nb oxide films is very close, but not equal, to that of an ideal capacitor, in agreement with the need of using CPE as a model for the system. Whenever an acid is used as the forming electrolyte,

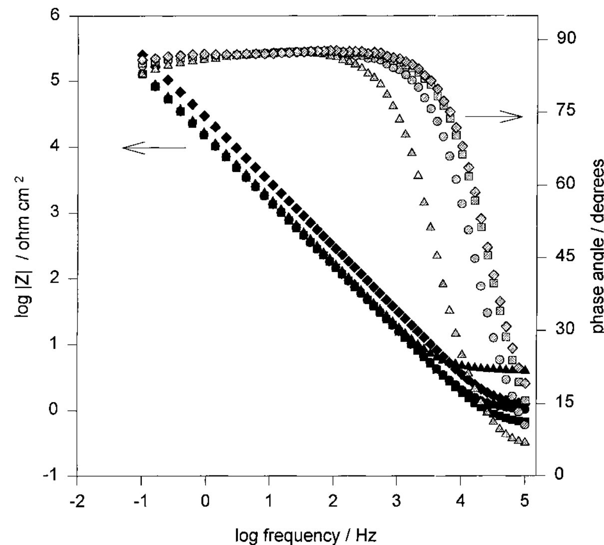

Fig. 7. Comparative impedance spectra for Nb oxide films grown in different forming electrolytes. Legend: (●) H_2SO_4, (■) HNO_3, (▲) H_3PO_4 and (♦) NaOH. (Nb/Nb_2O_5, $E_f = 2$ V).

Table 2. Values for the CPE parameter n

Electrolyte	*Ta/Ta_2O_5*	*Nb/Nb_2O_5*
H_2SO_4	0.9896 ± 0.0003	0.9698 ± 0.0004
HNO_3	0.9894 ± 0.0004	0.9618 ± 0.0007
H_3PO_4	0.9883 ± 0.0004	0.9601 ± 0.0009
NaOH	0.9857 ± 0.0002	0.9842 ± 0.0004

anodic oxides grown on Ta turn out to be a better dielectric material than anodic oxides on Nb, as evidenced by the higher n and ϕ values obtained for the former. These results are in good agreement with studies on oxide stability in aggressive media [23]. Data for n and ϕ reveal that the dielectric nature of the oxide films formed both on Ta and on Nb in NaOH is very similar.

Figures 6 and 7 show EIS results for oxide films grown up to the same final formation potential, in each of the electrolytes studied. No matter which solution is used to form a film, the general characteristics of the log $|Z|$ against log f and ϕ against log f plots are the same. The greater α value for the Ta and Nb oxides grown in NaOH and, hence, their higher film thickness, contributes to their greater $|Z|$ value observed in the impedance plots.

3.3. *Electrical parameters*

Fitting EIS data according to an equivalent circuit model also gives oxide resistance (R_L) and oxide capacitance (C_L) values. From the variation of these electrical parameters with final formation potential, average values of the oxide resistivity (ρ) and the oxide dielectric constant (ε_r) (or relative permittivity) are calculated [39].

Combining the thickness (d) – final formation potential (E_f) relationship (4) derived from the high field law [15]

$$d = d_0 + \alpha(E_f - E_0) \quad (4)$$

with the capacitance and resistance equations (5, 6) for a parallel-plate capacitor

$$\frac{C_L}{A} = \frac{\varepsilon_0 \varepsilon_r r}{d} \quad (5)$$

$$R_L A = \frac{\rho d}{r} \quad (6)$$

yields

$$\frac{A}{C_L} = \frac{d_0 - \alpha E_0}{\varepsilon_0 \varepsilon_r r} + \frac{\alpha}{\varepsilon_0 \varepsilon_r r} E_f \quad (7)$$

Table 3. Values for phase angle ϕ/degrees (at log $f < 3$)

Electrolyte	*Ta/Ta_2O_5*	*Nb/Nb_2O_5*
H_2SO_4	88.6 ± 0.3	87.1 ± 0.2
HNO_3	88.7 ± 0.4	86.7 ± 0.3
H_3PO_4	88.5 ± 0.3	86.6 ± 0.2
NaOH	87.3 ± 0.4	87.4 ± 0.4

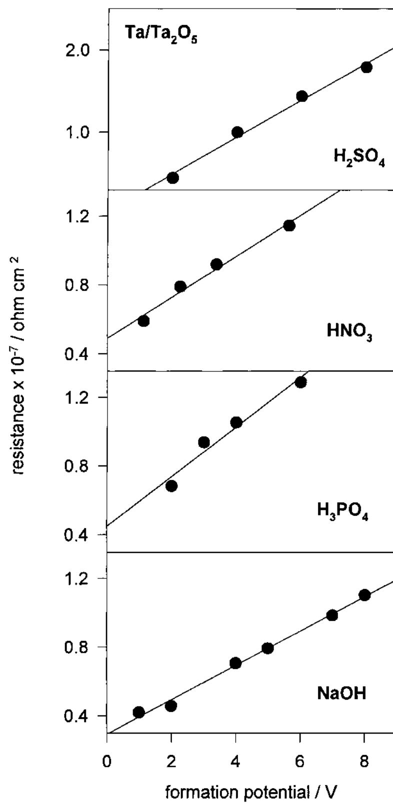

Fig. 8. Oxide resistance as a function of final formation potential for Ta oxide films. Solid straight lines represent the least-squares fit to Equation 8.

and

$$R_{\mathrm{L}}A = \rho\frac{d_0 - \alpha E_0}{r} + \frac{\rho\alpha}{r}E_{\mathrm{f}} \quad (8)$$

where d_0 is the thickness of the spontaneously grown oxide layer, E_0 is the potential at which oxide growth

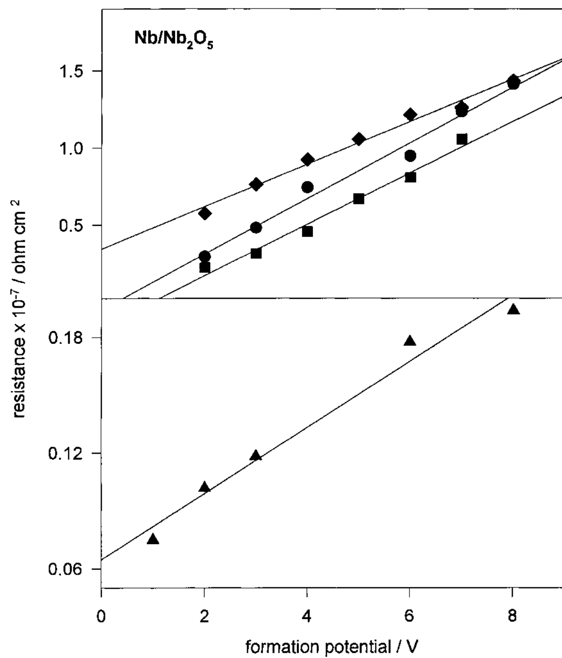

Fig. 9. Oxide resistance as a function of final formation potential for Nb oxide films. Solid straight lines represent the least-squares fit to Equation 8. Legend: (●) H_2SO_4, (■) HNO_3, (♦) NaOH and (▲) H_3PO_4.

Table 4. Values for the average oxide resistivity $\rho/10^{12}\ \Omega$ cm

Electrolyte	*Ta/Ta$_2$O$_5$*	*Nb/Nb$_2$O$_5$*
H_2SO_4	17 ± 2	8.7 ± 0.6
HNO_3	10 ± 2	6.9 ± 0.9
H_3PO_4	12 ± 3	1.1 ± 0.1
NaOH		

begins, $\varepsilon_0 = 8.85 \times 10^{-14}$ F cm^{-1}, A is the geometric area, and r is the roughness factor. In Equation 7 the contribution from the double layer capacitance is neglected [15, 19].

The variation of the oxide resistance with final formation potential is shown in Fig. 8 for Ta and in Fig. 9 for Nb. From equation 8 an R_{L} against E_{f} plot should be a straight line whose slope furnishes the values for ρ. These are presented in Table 4. The order of magnitude obtained is in good agreement with the electronic nature of these films, which behave like either wide bandgap semiconductors or insulators [15, 25, 43, 44]. The lower resistivity of the films formed on Nb in H_3PO_4 may be due to a relatively high defect concentration induced by anion incorporation from the electrolyte [45].

Figure 10 shows the reciprocal capacitance as a function of final formation potential for Ta oxide films. The relation should be a straight line according to Equation 7. The values for ε_r in Table 5, obtained from the slopes, are similar to those reported in the literature [15, 19] and agree with the results of Randall, who observed a decrease in ε with the amount of phosphate incorporated into Ta_2O_5 [17].

The variation of the reciprocal capacitance with final formation potential for Nb oxide films is presented in Fig. 11. The dependence of $1/C$ with E_{f} is linear in the whole potential range investigated only in the case of NaOH as forming electrolyte. Two

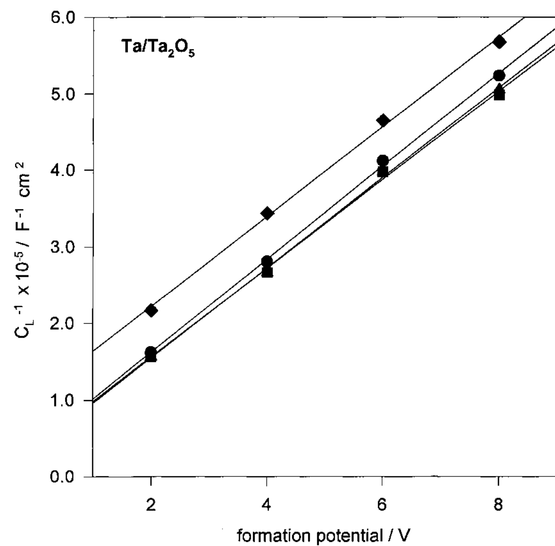

Fig. 10. Oxide reciprocal capacitance as a function of formation potential for Ta oxide films. Solid straight lines represent the least-squares fit to Equation 7. Legend: (●) H_2SO_4, (■) HNO_3, (▲) H_3PO_4 and (♦) NaOH.

Table 5. Values for the average oxide dielectric constant ε_r

Electrolyte	*Ta/Ta$_2$O$_5$*	*Nb/Nb$_2$O$_5$*
H_2SO_4	26 ± 1	119 ± 7
HNO_3	27 ± 1	120 ± 8
H_3PO_4	25 ± 1	89 ± 5
NaOH	29 ± 2	49 ± 3

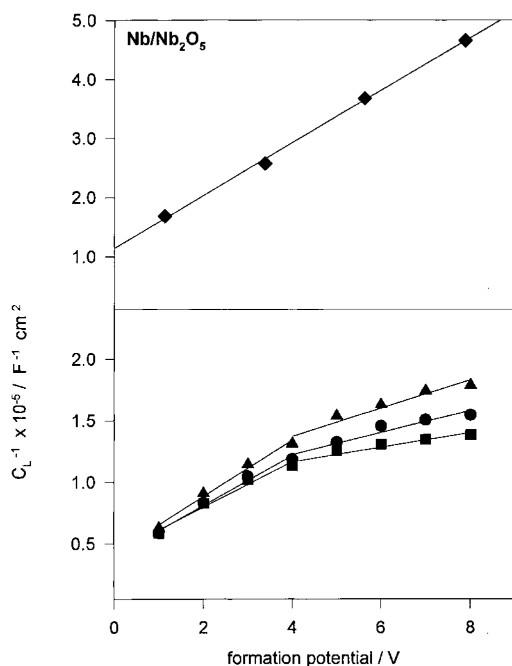

Fig. 11. Oxide reciprocal capacitance as a function of formation potential for Nb oxide films. Solid straight lines represent the least-squares fit to Equation 7. Legend: (♦) NaOH, (●) H_2SO_4, (■) HNO_3 and (▲) H_3PO_4.

straight lines of different slopes are found for the oxides grown in acidic solutions, one in the range 0–4 V and the other in the range 4–8 V. The change in the slope values may be associated with a variation of ε_r; notwithstanding, the reason for the slope breakdown could not be clearly deduced from the experimental results hitherto obtained. A slope breakdown in $1/C_L$ against E_f curves was reported for Ta oxide films by Kerrec *et al.* [19]; this result was explained on the basis of the influence of a substoichiometric oxide on the film dielectric constant. However, oxide films grown on chemically polished Nb substrates were found to exhibit only the pentoxide stoichiometry [1]. The ε_r values in Table 5 correspond to the range 0–4 V. The value of ε_r for NaOH compares well with previous results [13]. The notably high ε_r values obtained for the oxides formed in the acidic electrolytes are interpreted on the basis of a possible proton incorporation [31, 46, 47], as a result of which the electronic properties of Nb oxide films change from those of a wide bandgap semiconductor into those of a degenerate semiconductor [31]. For amorphous oxide semiconductors, an increase in ε_r is usually related to and increase in conductivity [36], and the latter is known to occur when the above electronic structural transformation takes place [48].

4. Conclusions

(i) The current–potential profiles reveal that the efficiency of anodic oxide growth on Ta and on Nb may be considered 100%, even in the case of nitric acid, a forming electrolyte which usually behaves as a corrosive species for other valve metals.
(ii) The dielectric behaviour of Ta/Ta$_2$O$_5$/electrolyte and Nb/Nb$_2$O$_5$/electrolyte systems approaches that of an ideal capacitor dielectric. EIS results indicate that the most pronounced deviations correspond to oxide films formed on Nb in acidic solutions. In this case, relatively unusual dielectric properties are observed, probably owing to an incorporation of protons from the electrolyte into the film.
(iii) The lower ρ and higher ε_r values for Nb oxide films with respect to Ta oxide films are in good agreement with the difference in the bandgap energy – $E_g(Nb_2O_5) = 3.4$ eV, $E_g(Ta_2O_5) = 4.3$ eV, in agreement with a trend observed throughout a variety of semiconductors.

Acknowledgements

Financial support from the Consejo Nacional de Investigaciones Científicas y Técnicas (CONICET) of Argentina, the Secretaría de Ciencia y Tecnología (SECyT) of the Universidad Nacional de Córdoba, and the Consejo de Investigaciones Científicas y Tecnológicas de Córdoba (CONICOR) is gratefully acknowledged. GEC thanks CONICET for the fellowship granted. The authors are grateful to the Alexander von Humboldt Foundation for the donation of an analyser ZAHNER IM5D. The authors thank Dr. E. M. Patrito for helpful suggestions and Miss L. P. Falcón for language assistance.

References

[1] J. J. Randall Jr., W. J. Bernard and R. R. Wilkinson, *Electrochim. Acta* **10** (1965) 183.
[2] J. P. S. Pringle, *J. Electrochem. Soc.* **120** (1973) 398.
[3] F. Climent, R. Capellades and J. Gil, *ibid.* **133** (1986) 959.
[4] T. B. Tripp and K. B. Foley, *ibid.* **137** (1990) 2528.
[5] V. Kadary and N. Klein, *ibid.* **127** (1980) 139.
[6] I. Montero, M. Fernández and J. M. Albella, *Electrochim. Acta* **32** (1987) 171.
[7] I. Montero, J. M. Albella and J. M. Martínez-Duart, *J. Electrochem. Soc.* **132** (1985) 976.
[8] K. C. Kalra and P. Katyal, *J. Appl. Electrochem.* **21** (1991) 729.
[9] R. E. Pawel, J. Pemsler and C. A. Evans Jr., *J. Electrochem. Soc.* **119** (1972) 24.
[10] W. Wilhelmsen, *Electrochim. Acta.* **33** (1988) 63.
[11] L. Young, Ta-Ming Yang and C. Backhouse, *J. Electrochem. Soc.* **142** (1995) 3479.
[12] M. A. Biason Gomes, S. Onofre, S. Juanto and L.O. de S. Bulhoes, *J. Appl. Electrochem.* **21** (1991) 1023.
[13] T. Hurlen, H. Bentzen and S. Hornkjol, *Electrochim. Acta* **32** (1987) 2623.
[14] S. Hornkjol, *ibid.* **36** (1991) 1443.
[15] V. A. Macagno and J. W. Schultze, *J. Electroanal. Chem.* **180** (1984) 157.

[16] F. Climent, R. Capellades and J. Gil, *Electrochim Acta* **38** (1993) 285.
[17] J. J. Randall Jr., *ibid.* **20** (1975) 663.
[18] A. Resetic and B. Jaric, *J. Appl. Electrochem.* **20** (1990) 768.
[19] O. Kerrec, D. Devilliers, H. Groult and M. Chemla, *Electrochim. Acta.* **40** (1995) 719.
[20] W. A. Badawy and Kh. M. Ismail, *ibid.* **38** (1993) 2231.
[21] A. G. Gad Allah, W. A. Badawy and H. H. Rehan, *J. Appl. Electrochem.* **19** (1989) 768.
[22] A. G. Gad Allah, *ibid.* **21** (1991) 346.
[23] F. M. Al-Kharafi and W. A. Badawy, *Electrochim. Acta.* **40** (1995) 2623.
[24] J. W. Schultze and V. A. Macagno, *ibid.* **31** (1986) 355.
[25] K. E. Heusler and M. Schulze, *ibid.* **20** (1975) 237.
[26] F. Di Quarto, S. Piazza, R. D'Agostino and C. Sunseri, *ibid.* **34** (1989) 321.
[27] W. A. Badawy, *J. Appl. Electrochem.* **20** (1990) 139.
[28] K. Miyairi, *Thin Solid Films*, **177** (1989) 1.
[29] C. G. Matthews, J. L. Ord and W. P. Wang, *J. Electrochem. Soc.* **130** (1983) 285.
[30] A. Duparre, E. Welsch, H. G. Walther, H. J. Kuhn and G. Schirmer, *J. Physique.* **48** (1987) 1155.
[31] R. Cabanel, J. Chaussy, J. Mazuer, G. Delabouglise, J. C. Joubert, G. Barral and C. Montella, *J. Electrochem. Soc.* **137** (1990) 1444.
[32] T. Maruyama and T. Kanagawa, *J. Electrochem. Soc.* **141** (1994) 2868.
[33] T. Maruyama and S. Arai, *Appl. Phys. Lett.* **63** (1993) 869.
[34] L. Young, *Trans. Faraday Soc.* **51** (1955) 1250.
[35] M. J. Chappell and J. S. L. Leach, *in* 'Passivity of Metals' (edited by R.P. Frankenthal and J. Kruger), The Electrochemical Society, Princeton, NJ (1978), p. 1003.
[36] L. Young, 'Anodic Oxide Films', Academic Press, New York (1961)
[37] M. J. Dignam, *in* 'Comprehensive Treatise of Electrochemistry' (edited by J. O'M. Bockris, B. E. Conway, E. Yeager and R. E. White), Vol. 4, Plenum New York (1981), p. 247.
[38] E. M. Patrito, R. M. Torresi, E. P. M. Levia and V. A. Macagno, *J. Electrochem. Soc.* **137** (1990) 524.
[39] M. J. Esplandiu, E. M. Patrito and V.A. Macagno, *J. Electroanal. Chem.* **353** (1993) 161.
[40] J. R. Macdonald, *ibid.* **223** (1987) 25.
[41] Idem, 'Impedance Spectroscopy', John Wiley & Sons, New York (1987).
[42] K. Juttner, J.W. Lorenz, M. W. Kending and F. Mansfeld, *J. Electrochem. Soc.* **135** (1988).
[43] 'CRC Handbook of Chemsitry and Physics', CRC Press, Boca Raton, (1992).
[44] J. W. Schultze and L. Elfenthal, *J. Electroanal. Chem.* **204** (1986) 153.
[45] E. M. Patrito and V. A. Macagno, *ibid.* **375** (1994) 203.
[46] M. A. B. Gomes and L.O. de S. Bulhoes, *Electrochim. Acta.* **35** (1990) 765.
[47] R. Cabanel, G. Barral, J. P. Diard, B. Le Gorrec and C. Montella, *J. Appl. Electrochem* **23** (1993) 93.
[48] P. S. Kireev, 'Semiconductor Physics', MIR Publishers, Moscow (1978).